



**HAL**  
open science

## Caryophyllene as a Precursor of Cross-Linked Materials

Etienne Grau, Anderson M. M. S. Medeiros, Cédric Le Coz

► **To cite this version:**

Etienne Grau, Anderson M. M. S. Medeiros, Cédric Le Coz. Caryophyllene as a Precursor of Cross-Linked Materials. ACS Sustainable Chemistry & Engineering, 2020, 10.1021/acssuschemeng.9b07413 . hal-02471294

**HAL Id: hal-02471294**

**<https://hal.science/hal-02471294>**

Submitted on 7 Feb 2020

**HAL** is a multi-disciplinary open access archive for the deposit and dissemination of scientific research documents, whether they are published or not. The documents may come from teaching and research institutions in France or abroad, or from public or private research centers.

L'archive ouverte pluridisciplinaire **HAL**, est destinée au dépôt et à la diffusion de documents scientifiques de niveau recherche, publiés ou non, émanant des établissements d'enseignement et de recherche français ou étrangers, des laboratoires publics ou privés.

# *Caryophyllene* as a precursor of cross-linked materials

*Anderson M. M. S. Medeiros,<sup>†</sup> Cédric Le Coz,<sup>†</sup> Etienne Grau<sup>†\*</sup>*

<sup>†</sup> Univ. Bordeaux, CNRS, Bordeaux INP, LCPO, UMR 5629, F-33600, 16, Avenue Pey Berland, 33607, Pessac, France.

\* [etienne.grau@enscbp.fr](mailto:etienne.grau@enscbp.fr)

**Abstract:** This paper aims at the synthesis of a new type of elastomers from caryophyllene. The adopted strategy was to cross-link the polycaryophyllene, which was synthesized by ring-opening metathesis polymerization (ROMP). The polycaryophyllene obtained showed  $M_n = 2 \times 10^4 \text{ g.mol}^{-1}$  ( $\mathcal{D} = 1.5$ ) with a glass transition temperature ( $T_g$ ) of  $-35 \text{ }^\circ\text{C}$ . On the first hand, thermal cross-linking was performed in the presence of organic peroxides or sulfur system. On the second hand, thiol-ene coupling initiated by UV-light at room temperature was also investigated as an alternative pathway to cross-link the polycaryophyllene. The materials obtained were analyzed by TGA, DSC, and DMA. The  $T_g$  of cross-linked polycaryophyllene could be easily modulated from  $-35 \text{ }^\circ\text{C}$  to a range between  $-25$  and  $10 \text{ }^\circ\text{C}$  by changing the type of cross-linking agent. The curing process led to the improvement of thermal stability ranging from  $200 \text{ }^\circ\text{C}$  to around  $340 \text{ }^\circ\text{C}$ . Finally, the network storage modulus varied from 1 to 100 MPa at room temperature.

**Keywords:** terpene; sesquiterpene; ROMP; elastomer; vulcanization; click-chemistry; solvent-free.

## Introduction

New strategies to develop materials from renewable feedstock have been continuously sought as greener alternatives to commercial oil-based materials. There is a significant interest in polymeric materials, taking into consideration their wide range of applications, especially for elastomers. The elastomers market has witnessed significant growth in the global production in recent years, with an estimated increase in revenue from current US\$ 80.73 billion to close to US\$ 104.17 billion by 2026.<sup>1,2</sup> The adoption of vulcanized thermoplastics (TPV) in various application sectors has led to this development. Among several categories of thermoplastics, the natural rubbers (NR) emerge as a major players. The NR segment plays an important role in the TPV global market since the NR is one of the most used thermoplastic thanks to their versatility.<sup>2</sup> Due to their properties such as high thermal stability, good chemical resistance, high tensile strength, low shrinkage, and greater design flexibility, they can be employed as devices and/or tools for automotive, medical, consumer goods, industrial, and other applications.<sup>3,4</sup> In the framework of looking for an alternative to oil-based consumer goods, an important number of research groups have concentrated their studies and described the synthesis of vegetable-oil-based thermoplastics, such as polyester, polyurethanes, polyamides, and many other bio-based polymers.<sup>4-10</sup> Terpenes and terpenoides have drawn considerable attention as potential starting precursors in the synthesis of elastomers.<sup>11-18</sup> Studies on the synthesis of elastomers from pinene, myrcene, and limonene<sup>19-24</sup> can be readily found in the scientific literature and some commercially available resins and adhesives (e.g. Piccolyte®) derived from polypinenes are already reported. However, there is little exploitation of sesquiterpenes by the scientific community.<sup>25,26</sup> Among molecules defined as sesquiterpenes, caryophyllene and humulene stand out, since these molecules are made of interesting structural elements. These molecules are found in many essential oils such

as rosemary, cannabis sativa, hops, and mostly clove oil.<sup>27-29</sup> With a worldwide production of 190 million metric tons per years, clove oil is the main source of caryophyllene. Indeed, clove oil primary use is to extract the eugenol from the oil by distillation. Caryophyllene, which represents around 10% of the clove oil, is a waste in this process and is usually burned.

All these led to the fact that caryophyllene being one of the cheapest and most abundant sesquiterpene. Moreover, from a chemical point of view, caryophyllene is a versatile and significant molecule due to a bicyclic and a cyclobutane rings as well as unsaturated bonds present in its chemical structure.<sup>28</sup> Thanks to them, the caryophyllene can be easily modified by attaching different moieties to its backbone chain. Moreover caryophyllene is, to the best of our knowledge, the only readily available bio-based molecule that can be polymerized by ring-opening metathesis polymerization (ROMP) leading to polycaryophyllene (PCar).<sup>30</sup> PCar exhibits two carbon-carbon double bonds in its structure which can be further used to cross-link it.

Keeping in mind this context, the present research has aimed to the cross-linking of polycaryophyllene by using different routes and investigating the thermo-mechanical properties of the newly produced cross-linked bio-based elastomer. Two main pathways have been considered to reach three dimensional cross-linked polycaryophyllene: i) thermal pathways: in the presence of organic peroxides [benzoyl peroxide (BPO) or dicumyl peroxide (DCP)], or by classical vulcanization based on sulfur system (SS) and ii) via UV light initiated thiol-click reactions at room temperature (see diagram in Figure 1) using different dithiols, such as 1,2-ethanedithiol (EDT), 1,4-butanedithiol (BDT), 1,6-hexanedithiol (HDT), and 1,10-decanedithiol (DDT). As far as we know, this is the first study about the cross-linking of polycaryophyllene.

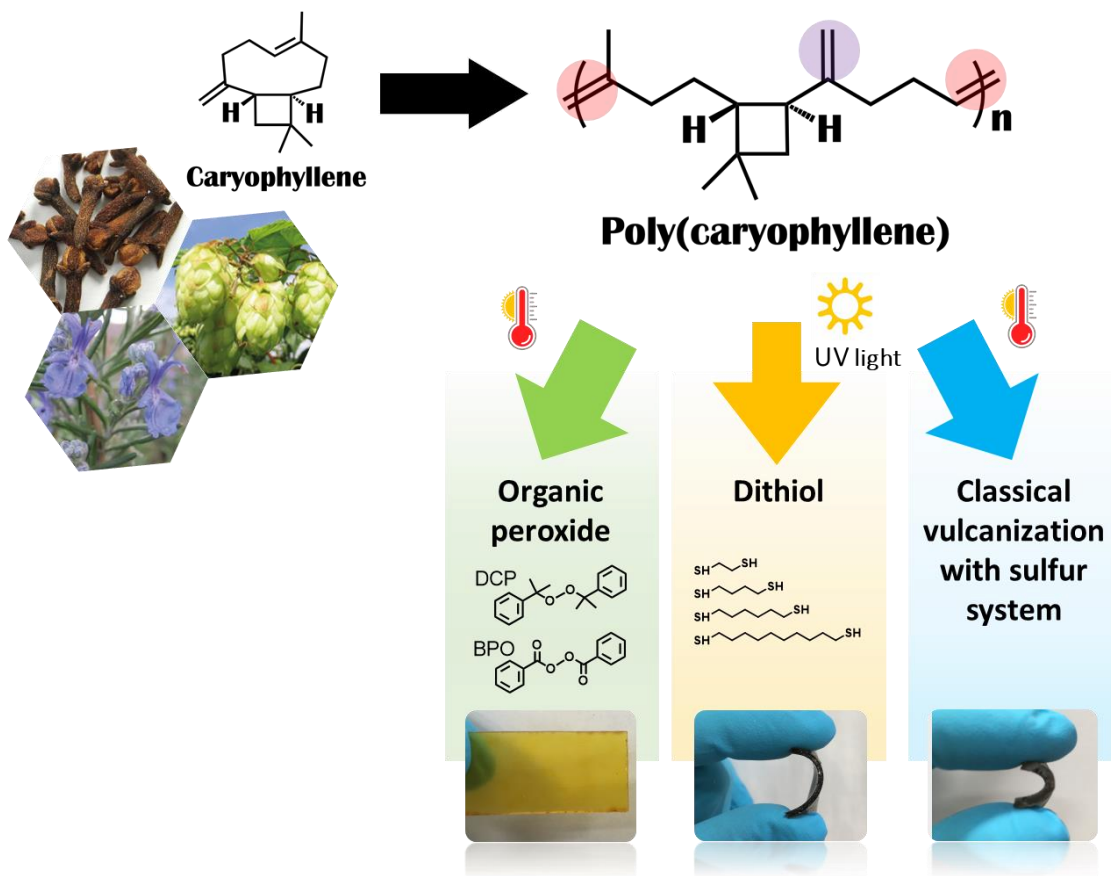


**Figure 1** Scheme of caryophyllene ROMP and subsequent cross-linking of polycaryophyllene by different pathways. Credit: hop picture by Hagen Graebner [CC BY-SA 2.5](https://creativecommons.org/licenses/by-sa/2.5/), rosemary picture by Margalob [CC BY-SA 4.0](https://creativecommons.org/licenses/by-sa/4.0/)

## Results & Discussion

ROMP of caryophyllene was performed by dissolving Grubbs' 2nd Generation catalyst ((tricyclohexylphosphine) (1.3-dimesitylimidazolidine-2-ylidene) benzyldeneruthenium dichloride) (0.2 mol % to monomer) in caryophyllene without any solvent at room temperature for 24 hours under  $N_2$  atmosphere. The obtained polycaryophyllene ( $M_n = 23 \text{ kg}\cdot\text{mol}^{-1}$ ,  $D = 1.5$ ) was used without any further purification for thermal cross-linking or UV cross-linking (see Figure S1-S6). For thermal cross-linking, the polymer was homogenized with the selected cross-linker and

the mixture was kept at 160 °C under 30 bar for 1 hour in a machine press. For UV-light initiated cross-linking, the polycaryophyllene was mixed with dithiol and IRGARCUR 2959 (photo-cross-linker), placed into a Teflon mold and left in a UV-reactor ( $\lambda = 320\text{-}380$  nm) for 4 hours.

To confirm the cross-linking, the gel fractions were quantified by extraction in THF at 50 °C for 48 hours. The resulted gel fractions were 65 %, 90 %, and 72% for BPO, DCP, and SS respectively, as summarized in Table 1. The gel fraction appears to be limited for BPO cross-linking at 65% since even an increase of the curing temperature to 180 °C does not improve the gel fraction (see Table S1).

Obtaining a higher amount of gel fraction with DCP compared to with BPO was already identified in other studies.<sup>31,32</sup> Indeed, DCP is the most frequently used cross-linking agent since it is an organic peroxide which is more selective to vinyl moieties than benzoyl peroxide.<sup>33,34</sup> The ability of cumyloxy radical from DCP to react with non-activated vinyl moieties in a free-radical cross-linking pathway *via* H abstraction may be a possible explanation of its higher reactivity compared to BPO.<sup>35</sup> Additionally, the cumyloxy radical can undergo  $\beta$ -scission resulting in radical fragments (methyl radical and acetophenone) with high mobility.<sup>36</sup> Furthermore, the unsaturated bonds are not easily accessible by benzoyloxy radicals due to the steric hindrance around double bonds as the increase of formation of cross-linked networks.<sup>29</sup> The SEC analysis of the BPO soluble fraction testified to the presence of oligomers (see Figure S7,  $M_n = 320$  g.mol<sup>-1</sup>,  $D = 1.5$ ) which indicated that some polymer backbone cleavage also takes place during the cross-linking. In the case of the sulfur system, the soluble fraction is mainly constituted of the accelerator and the catalyst used. Finally, the IR analysis of the materials obtained (see Figure S8) shows that whatever the cross-linker, the vibration characteristics of the carbon-carbon double bond (i.e.

=CH<sub>2</sub> bending 887 cm<sup>-1</sup>, C=C stretching at 1645 cm<sup>-1</sup>, C-H stretching at 3115 cm<sup>-1</sup>) are still present indicating a crosslinking by hydrogen abstraction mechanisms.

In order to confirm the occurrence of cross-linking reactions, on-line rheology measurements were carried out, they are shown in Figure 2. The visco-elastic analysis also provided an estimation of the initial temperature of the cross-linking process.

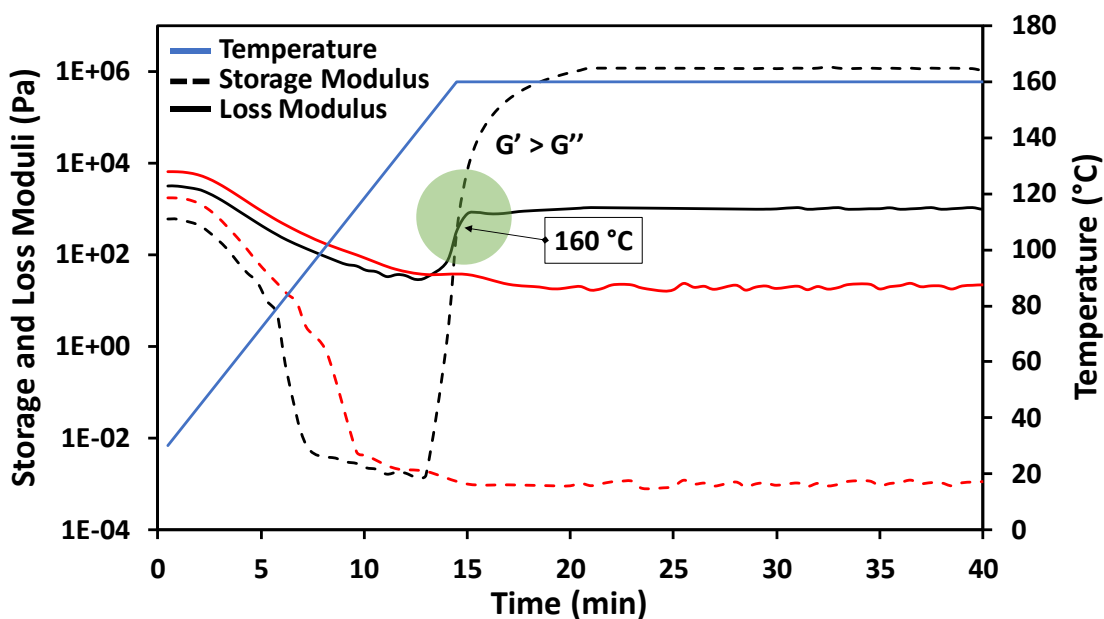


**Figure 2.** Rheology curves of polycaryophyllene with (black) or without (red) DCP, and temperature (blue). The solid line represents the loss modulus ( $G''$ ) and dashed line corresponds to storage modulus ( $G'$ ).

As expected, polycaryophyllene in the absence of a crosslinker behaves as a liquid for temperatures up to 160°C with the loss modulus ( $G''$ ) higher than the storage modulus ( $G'$ ). Classically, as the temperature increases, both moduli continuously decrease and no cross-linking reaction takes place at 160°C since no change in moduli was observed over time.

In the presence of DCP, a shoot up in moduli is clearly observed with a gel point (intersection point) at 160°C. Similar curves were obtained for the curing of polycaryophyllene with BPO and SS (see Figure S9-10) with gel points occurring at 118°C and 160°C respectively and are in agreement with DSC online curing curves (Figure S11-12).

After the gel point, both loss and storage moduli reached constant plateaus and no more significant changes are observed. The magnitude of storage modulus increased up to 1.2 MPa, 40, and 60 kPa and the loss modulus to 0.6, 0.5, and 0.5 kPa respectively for polycaryophylenes cross-linked by DCP, BPO, and sulfur system.

Concerning the UV cross-linking by thiol-ene coupling, the soluble fraction remains between 0% and 11% depending on the dithiol used (see Table 1). Interestingly, when the cross-linking is performed with 0.5 eq. of thiol per carbon-carbon double bond (db), a slight improvement of the gel fraction is observed compared to the materials synthesized with 1 eq of thiol per db (see Table S2). This may be due to the presence of remaining free dithiol in the soluble fraction. IR analysis of the polycaryophyllene obtained with 0.5 eq. of thiol per db shows no regioselectivity of the thiol-ene addition since the bands which are characteristic of the two carbon-carbon double bonds decrease (see Figure S13). For 1 eq. of thiol per db, double bonds appear to have totally disappeared whatever the dithiols used (see Figure S14). However, in all cases with 1 eq of thiol per db, IR spectra show a broad peak around 3400  $\text{cm}^{-1}$  which confirmed the presence of remaining thiols in the materials.

To obtain further information about cross-linked polycaryophylenes, TGA and DSC measurements were performed in order to investigate their thermal properties, as shown in Figure 3-4 and Table 1.

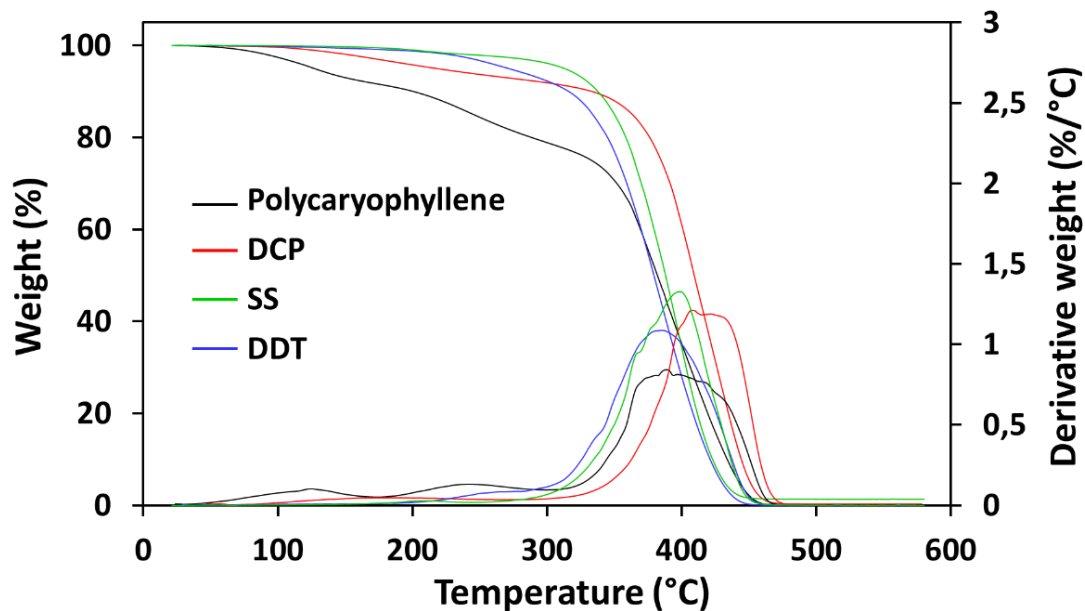


**Figure 3.** TGA and DTG curves of polycaryophyllene cross-linked by using different routes

**Table 1.** Thermo-mechanical properties of cross-linked polycaryophyllenes.

|                               | Entry             | Insoluble Fraction <sup>a</sup> (%) | $T_g^b$ (°C) | $T_{10\%}^c$ (°C) | $\text{Tan}\delta^e$ (°C) | $E'^c$ (MPa) | Cross-linking degree <sup>f</sup> ( $10^3 \text{ mol.m}^{-3}$ of elastomer) |
|-------------------------------|-------------------|-------------------------------------|--------------|-------------------|---------------------------|--------------|---|
|                               | Polycaryophyllene | 0                                   | -35          | 200               | NA                        | NA           | 0   |
| Organic Peroxide              | Pcar/DCP          | 90                                  | 12           | 335               | 4                         | 28           | 11  |
|                               | Pcar/BPO          | 65                                  | -6           | 245               | -12                       | 0.7          | 0.4   |
| Vulcanization                 | Pcar/SS           | 72                                  | -9           | 315               | -5                        | 0.9          | 0.3   |
|                               | Pcar/EDT          | 100                                 | -22          | 338               | -16                       | 0.9          | 1.1   |
| Dithiol (0.5 equiv. SH to db) | Pcar/BDT          | 100                                 | -16          | 325               | -17                       | 8.2          | 3.1   |
|                               | Pcar/HDT          | 95                                  | -15          | 332               | -15                       | 2.0          | 0.8   |
|                               | Pcar/DDT          | 98                                  | -6           | 336               | -2                        | 4.6          | 1.9   |

<sup>a</sup> Extraction in THF at 50 °C for 48 h ( $\text{IF} = m_d/m_0$  with  $m_d$  the mass of the dried sample and  $m_0$  the mass of the sample before extraction by THF); <sup>b</sup> Obtained by DSC; <sup>c</sup> Obtained by TGA; <sup>e</sup> Obtained by DMA; <sup>f</sup> Determined using the rubber-like elasticity theory.

According to TGA (see Figure 3 and Figure S15-S16), the crosslinking of polycaryophyllene increases its thermal stability. Indeed, the temperature of 10% of degradation ( $T_{10\%}$ ) for polycaryophyllene is around 200 °C. After cross-linking, the  $T_{10\%}$  take place at temperature ranging from 310 to 340 °C.

DSC measurements were performed to evaluate the effect of newly formed cross-linked structures on the glass transition temperatures ( $T_g$ ) of polycaryophyllene (See Figure 4 and Figure S17).

The  $T_g$  of cross-linked polycaryophyllene increased significantly compared to non-cross-linked polycaryophyllene ( $T_g = -35$  °C). The curing by DCP provided more rigidity to polycaryophyllene ( $T_g = 12$  °C) than the one by sulfur system ( $T_g = -9$  °C) or DDT ( $T_g = -6$  °C). Moreover the  $T_g$  of the network gradually increases with the chain length of the dithiol from -22°C for EDT to -6°C for DDT.

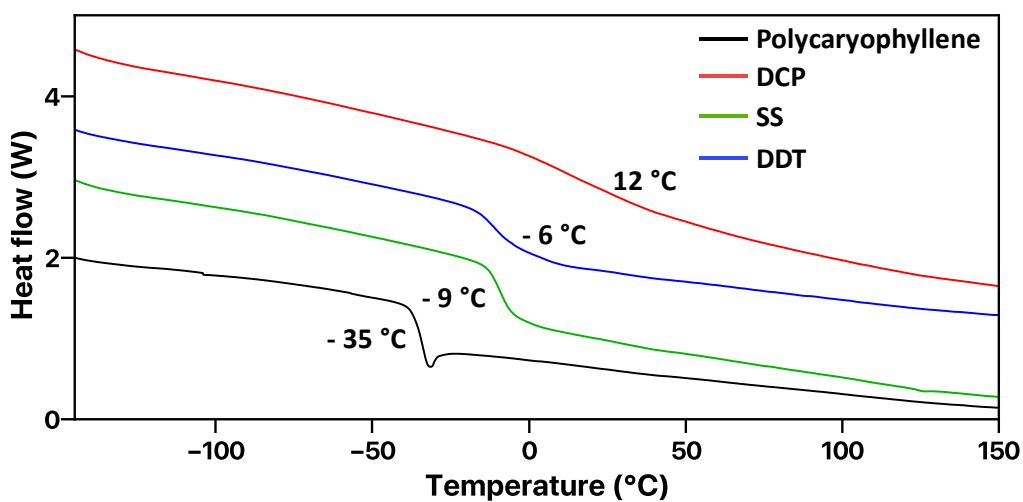


**Figure 4.** DSC Curves of cross-linked polycaryophyllene.

The mechanical properties of cross-linked polycaryophyllene were evaluated by dynamic mechanical analyses (DMA), displayed in Figure 5 and Figure S19.

The DMA curves show a typical behavior for cross-linked materials with a glassy plateau before the alpha transition temperature ( $T_{\alpha}$ ) followed by a rubbery zone after this point.

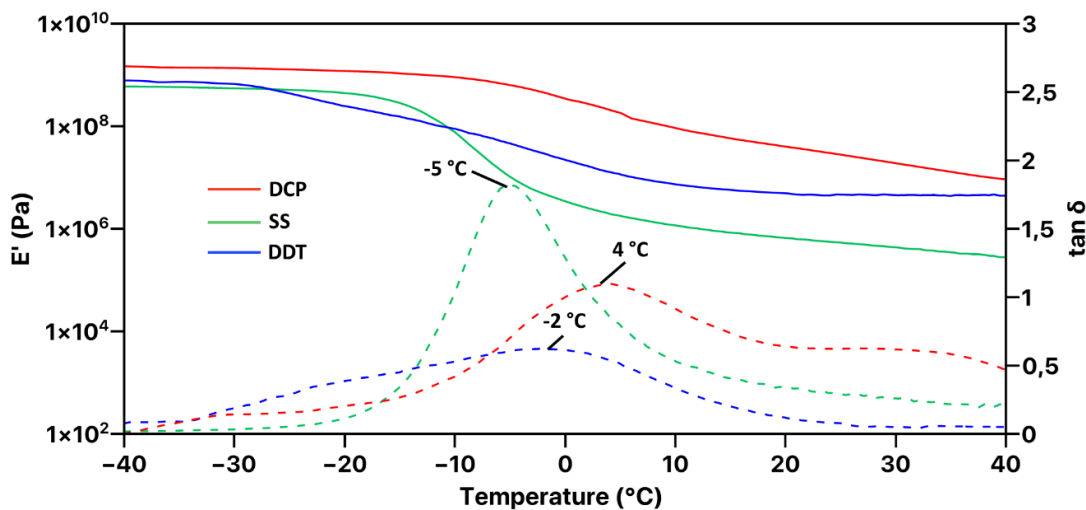


**Figure 5.** DMA analysis of cross-linked polycaryophyllene by DCP, DDT and SS. Storage modulus in solid line,  $\tan \delta$  in dashed line.

Polycaryophyllene crosslinked by DCP exhibits the highest glassy storage modulus (over 1 GPa). The  $T_{\alpha}$  values were 4 °C, -2 °C and -5 °C for Pcar/DCP, Pcar/DDT and Pcar/SS respectively (see Figure 5), and can be considered in agreement with the one obtained by DSC (12 °C, -6 °C and -9 °C respectively). Finally, the rubbery plateau confirms the cross-linking of the materials and its value is directly proportional to the cross-linking density. Polycaryophyllene crosslinked by DCP exhibits significantly higher storage modulus above glass transition temperature (28 MPa) compared to SS or BPO systems (0.7 and 0.9 MPa respectively) (see Table 1) or even DDT cross-linking (4.6 MPa).

Tensile tests were performed in order to obtain the values of tensile strength and elongation at break of cross-linked polycaryophyllene (see Figure S20). On the first hand, the cross-linked materials produced by BPO curing and vulcanization show elastomeric behaviors with a high value

of elongation at break (360 % and 187 %, respectively) and low Young moduli (1.7 and 2 MPa, respectively). On the other hand, in agreement with the DMA results, polycaryophyllene cross-linked by DDT exhibited much lower elongation at break (25 %) and higher Young modulus (40 MPa) compared to SS and BPO crosslinked materials.

## Conclusion

In conclusion, caryophyllene was polymerized by ROMP and the polymer obtained was cross-linked using different routes: organic peroxides, sulfur system or dithiol. Rheological analyses confirmed the occurrence of cross-linking reactions in agreement with the extractions by THF results. Swelling experiments showed that the polycaryophyllene was entirely cross-linked by DCP or dithiols with an insoluble fraction over 90%. Cross-linking by sulfur system resulted in a gel content of 72%.

The cross-linked materials were in-depth analyzed by TGA, DSC and DMA. Materials were obtained with  $T_g$  between  $-22\text{ }^{\circ}\text{C}$  and  $12\text{ }^{\circ}\text{C}$  with improved thermal stability compared to non-cross-linked polycaryophyllene ( $T_{10\%} > 300\text{ }^{\circ}\text{C}$ ). At room temperature ( $20\text{ }^{\circ}\text{C}$ ) storage modulus of the cross-linked polycaryophyllene were between 1 MPa to 100 MPa with elongation at break up to 360%.

Polycaryophyllene is a precursor of elastomers which can be cross-linked by various pathways. Its  $T_g$  of  $-35\text{ }^{\circ}\text{C}$  is close to the  $T_g$  of synthetic rubber such as EPDM, CR or NBR. To the best of our knowledge, it is the only polyterpenes in this range of temperature (see Table S3 in supporting information). Indeed, poly( $\beta$ -myrcene),<sup>20</sup> poly( $\beta$ -farsene)<sup>25</sup> exhibit  $T_g$  close to  $-70\text{ }^{\circ}\text{C}$  while poly(allocimene)<sup>18</sup> have a  $T_g$  of  $-17\text{ }^{\circ}\text{C}$ . Moreover with a production potential of 20 million metric

tons per year, caryophyllene is widely available and in quantity compatible with the synthetic rubber market which is estimated to 15 million metric tons per year.

## ACKNOWLEDGMENT

E.G. thanks Emergence@INC2019 for the research funding. The authors thank Equipex Xyloforest ANR-10-EQPX-16. The financial support from the CPER CAMPUSB project funded by the French state and the Région Nouvelle Aquitaine is gratefully acknowledged.

## REFERENCES

- (1) *Elastomers Market By Product Type (Thermoset Elastomers, Thermoplastic Elastomers), By End-Use Industry (Automotive, Healthcare, Consumer Goods, Construction, Oil & Gas, Others) - Growth, Future Prospect & Competitive Analysis, 2018-2026*, Credence Research, August 2018, <https://www.credenceresearch.com/report/elastomers-market>. (Accessed: 27 January 2020)
- (2) *Elastomers Market by Type (Thermoset (Natural Rubber, Synthetic Rubber (SBR, IIR, PBR, NBR, ACM, EPM)), and Thermoplastic (PEBA, SBC, TPO, TPU, TPV)), Application (Automotive, Consumer Goods, Medical, and Industrial) - Global Forecast to 2021*; MarketsandMarkets™ Research Private Ltd., January 2017, <https://www.marketsandmarkets.com/Market-Reports/elastomers-market-48929183.html>. (Accessed: 27 January 2020)

- (3) Biron, M. *Thermoplastics: Economic Overview (Chapter 3)*. In *Material Selection for Thermoplastic Parts*; William Andrew Publishing: Oxford, 2016; pp. 77–111. DOI 10.1016/B978-0-7020-6284-1.00003-9.
- (4) Mallick, P. K. *Thermoplastics and Thermoplastic–matrix Composites for Lightweight Automotive Structures*. In *Materials, Design and Manufacturing for Lightweight Vehicles*; Woodhead Publishing: University of Michigan-Dearborn, USA, 2010; pp. 174–207. DOI 10.1533/9781845697822.1.174.
- (5) Nekhavhambe, E.; Mukaya, H. E.; Nkazi, D. B. Development of Castor Oil–based Polymers: A Review. *J. Adv. Manuf. Process.* **2019**, *1*, e10030. DOI 10.1002/amp2.10030.
- (6) Zhang, C.; Garrison, T. F.; Madbouly, S. A.; Kessler, M. R. Recent Advances in Vegetable Oil-Based Polymers and Their Composites. *Top. Vol. Polym. Biomater.* **2017**, *71*, 91–143. DOI 10.1016/j.progpolymsci.2016.12.009.
- (7) Maisonneuve, L.; Lebarbé, T.; Grau, E.; Cramail, H. Structure–properties Relationship of Fatty Acid-Based Thermoplastics as Synthetic Polymer Mimics. *Polym. Chem.* **2013**, *4*, 5472–5517. DOI 10.1039/C3PY00791J.
- (8) Gandini, A.; Lacerda, T. M.; Carvalho, A. J. F.; Trovatti, E. Progress of Polymers from Renewable Resources: Furans, Vegetable Oils, and Polysaccharides. *Chem. Rev.* **2016**, *116*, 1637–1669. DOI 10.1021/acs.chemrev.5b00264.
- (9) Voirin, C.; Caillol, S.; Sadavarte, N. V.; Tawade, B. V.; Boutevin, B.; Wadgaonkar, P. P. Functionalization of Cardanol: Towards Biobased Polymers and Additives. *Polym. Chem.* **2014**, *5*, 3142–3162. DOI 10.1039/C3PY01194A.

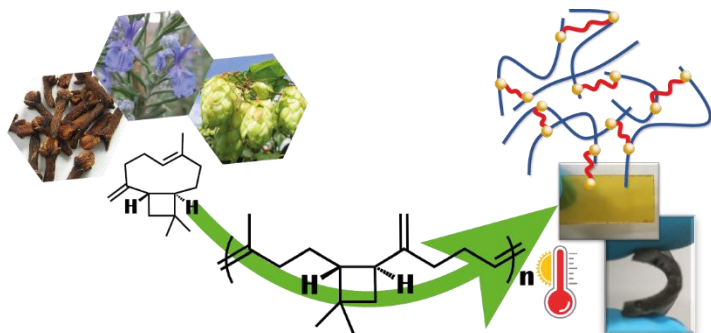
- (10) Holmberg, A. L.; Reno, K. H.; Wool, R. P.; Epps, I., Thomas H. Biobased Building Blocks for the Rational Design of Renewable Block Polymers. *Soft Matter* **2014**, *10*, 7405–7424. DOI 10.1039/C4SM01220H.
- (11) Sarkar, P.; Bhowmick, A. K. Sustainable Rubbers and Rubber Additives. *J. Appl. Polym. Sci.* **2018**, *135*, 45701-45734. DOI 10.1002/app.45701.
- (12) Thomsett, M. R.; Storr, T. E.; Monaghan, O. R.; Stockman, R. A.; Howdle, S. M. Progress in the Synthesis of Sustainable Polymers from Terpenes and Terpenoids. *Green Mater.* **2016**, *4*, 115–134. DOI 10.1680/jgrma.16.00009.
- (13) Winnacker, M.; Rieger, B. Recent Progress in Sustainable Polymers Obtained from Cyclic Terpenes: Synthesis, Properties, and Application Potential. *ChemSusChem* **2015**, *8*, 2455–2471. DOI 10.1002/cssc.201500421.
- (14) Wilbon, P. A.; Chu, F.; Tang, C. Progress in Renewable Polymers from Natural Terpenes, Terpenoids, and Rosin. *Macromol. Rapid Commun.* **2013**, *34*, 8–37. DOI 10.1002/marc.201200513.
- (15) Firdaus, M.; Montero de Espinosa, L.; Meier, M. A. R. Terpene-Based Renewable Monomers and Polymers via Thiol–Ene Additions. *Macromolecules* **2011**, *44*, 7253–7262. DOI 10.1021/ma201544e.
- (16) Noppalit, S.; Simula, A.; Ballard, N.; Callies, X.; Asua, J. M.; Billon, L. Renewable Terpene Derivative as a Biosourced Elastomeric Building Block in the Design of Functional Acrylic Copolymers. *Biomacromolecules* **2019**, *20*, 2241–2251. DOI 10.1021/acs.biomac.9b00185.

- (17) Miyaji, H.; Satoh, K.; Kamigaito, M. Bio-Based Polyketones by Selective Ring-Opening Radical Polymerization of  $\alpha$ -Pinene-Derived Pinocarvone. *Angew. Chem. Int. Ed.* **2016**, *55*, 1372–1376. DOI 10.1002/anie.201509379.
- (18) Sahu, P.; Sarkar, P.; Bhowmick, A. K. Synthesis and Characterization of a Terpene-Based Sustainable Polymer: Poly-Alloocimene. *ACS Sustain. Chem. Eng.* **2017**, *5*, 7659–7669. DOI 10.1021/acssuschemeng.7b00990.
- (19) Sarkar, P.; Bhowmick, A. K. Terpene-Based Sustainable Elastomers: Vulcanization and Reinforcement Characteristics. *Ind. Eng. Chem. Res.* **2018**, *57*, 5197–5206. DOI 10.1021/acs.iecr.8b00163.
- (20) Sarkar, P.; Bhowmick, A. K. Synthesis, Characterization and Properties of a Bio-Based Elastomer: Polymyrcene. *RSC Adv.* **2014**, *4*, 61343–61354. DOI 10.1039/C4RA09475A.
- (21) Sarkar, P.; Bhowmick, A. K. Terpene Based Sustainable Elastomer for Low Rolling Resistance and Improved Wet Grip Application: Synthesis, Characterization and Properties of Poly(Styrene-Co-Myrcene). *ACS Sustain. Chem. Eng.* **2016**, *4*, 5462–5474. DOI 10.1021/acssuschemeng.6b01038.
- (22) Raynaud, J.; Wu, J. Y.; Ritter, T. Iron-Catalyzed Polymerization of Isoprene and Other 1,3-Dienes. *Angew. Chem. Int. Ed.* **2012**, *51*, 11805–11808. DOI 10.1002/anie.201205152.
- (23) Satoh, K.; Sugiyama, H.; Kamigaito, M. Biomass-derived heat-resistant alicyclic hydrocarbon polymers: poly(terpenes) and their hydrogenated derivatives. *Green Chem.*, **2006**, *8*, 878-882 DOI 10.1039/B607789G.

- (24) Kamigaito, M.; Satoh, K. *Sustainable Vinyl Polymers via Controlled Polymerization of Terpenes*. In *Sustainable Polymers from Biomass*; John Wiley & Sons, Ltd, 2017; pp 55–90. DOI 10.1002/9783527340200.ch4.
- (25) Hashimoto, H.; Takeshima, H.; Nagai, T.; Uchiyama, M.; Satoh, K.; Kamigaito, M. Valencene as a Naturally Occurring Sesquiterpene Monomer for Radical Copolymerization with Maleimide to Induce Concurrent 1:1 and 1:2 Propagation. *Polym. Degrad. Stab.* **2019**, *161*, 183–190. DOI 10.1016/j.polymdegradstab.2019.01.025.
- (26) Yoo, T.; Henning, S. K. Synthesis and Characterization of Farnesene-Based Polymers. *Rubber Chem. Technol.* **2017**, *90*, 308–324. DOI 10.5254/rct.17.82683.
- (27) G. Collado, I.; R. Hanson, J.; J. Macías-Sánchez, A. Recent Advances in the Chemistry of Caryophyllene. *Nat. Prod. Rep.* **1998**, *15*, 187–204. DOI 10.1039/A815187Y.
- (28) Gertsch, J.; Leonti, M.; Raduner, S.; Racz, I.; Chen, J.-Z.; Xie, X.-Q.; Altmann, K.-H.; Karsak, M.; Zimmer, A. Beta-Caryophyllene Is a Dietary Cannabinoid. *Proc. Natl. Acad. Sci.* **2008**, *105*, 9099. DOI 10.1073/pnas.0803601105.
- (29) Chicca, A.; Caprioglio, D.; Minassi, A.; Petrucci, V.; Appendino, G.; Tagliatela-Scafati, O.; Gertsch, J. Functionalization of  $\beta$ -Caryophyllene Generates Novel Polypharmacology in the Endocannabinoid System. *ACS Chem. Biol.* **2014**, *9*, 1499–1507. DOI 10.1021/cb500177c.
- (30) Grau, E.; Mecking, S. Polyterpenes by Ring Opening Metathesis Polymerization of Caryophyllene and Humulene. *Green Chem.* **2013**, *15*, 1112–1115. DOI 10.1039/c3gc40300a.

- (31) Suyama, S.; Ishigaki, H.; Watanabe, Y.; Nakamura, T. Crosslinking of Polyethylene by Dicumyl Peroxide in the Presence of 2,4-Diphenyl-4-Methyl-1-Pentene. *Polym. J.* **1995**, *27*, 371–375. DOI 10.1295/polymj.27.371.
- (32) Wang, S.; Zhou, Q.; Liao, R.; Xing, L.; Wu, N.; Jiang, Q. The Impact of Cross-Linking Effect on the Space Charge Characteristics of Cross-Linked Polyethylene with Different Degrees of Cross-Linking under Strong Direct Current Electric Field. *Polymers* **2019**, *11*, 1149-1177. DOI 10.3390/polym11071149.
- (33) Baquey, G.; Moine, L.; Babot, O.; Degueil, M.; Maillard, B. Model Study of the Crosslinking of Polydimethylsiloxanes by Peroxides. *Polym. Blends Compos. Hybrid Polym. Mater.* **2005**, *46*, 6283–6292. DOI 10.1016/j.polymer.2005.05.078.
- (34) Dworakowska, S.; Le Coz, C.; Chollet, G.; Grau, E.; Cramail, H. Cross-Linking of Polyesters Based on Fatty Acids. *Eur. J. Lipid Sci. Technol.* **2019**, *121*, 1900264-1900276. DOI 10.1002/ejlt.201900264.
- (35) González, L.; Rodríguez, A.; Marcos, A.; Chamorro, C. Crosslink Reaction Mechanisms of Diene Rubber with Dicumyl Peroxide. *Rubber Chem. Technol.* **1996**, *69*, 203–214. DOI 10.5254/1.3538365.
- (36) Di Somma, I.; Marotta, R.; Andreozzi, R.; Caprio, V. Dicumyl Peroxide Thermal Decomposition in Cumene: Development of a Kinetic Model. *Ind. Eng. Chem. Res.* **2012**, *51*, 7493–7499. DOI 10.1021/ie201659a.

## For Table of Contents Use Only



### Synopsis

Caryophyllene was polymerized by ROMP, the polycaryophyllene obtained was then cross-linked leading to material exhibiting elastomeric-like properties

# Caryophyllene as a precursor of cross-linked materials

*Anderson M. M. S. Medeiros,<sup>†</sup> Cédric Le Coz,<sup>†</sup> Etienne Grau<sup>†\*</sup>*

The number of pages: 17

The number of Figures: 20

The number of Tables: 3

## **S1.** General experimental procedure

**Figure S1.** Schematic reaction of the polymerization of caryophyllene.

**Figure S2.** Chemical structures of different thiols.

**Figure S3.** Thiol-ene cross-linking reaction of polycaryophyllene.

**Figure S4** <sup>1</sup>H and <sup>13</sup>C NMR spectrum of caryophyllene in CDCl<sub>3</sub>.

**Figure S5** <sup>1</sup>H and <sup>13</sup>C NMR spectrum of polycaryophyllene in CDCl<sub>3</sub>.

**Figure S6.** Three different samples of Polycaryophyllene and Caryophyllene SEC profile.

**Table S1.** Gel fractions of cross-linked polycaryophyllene by BPO at varied temperatures.

**Figure S7.** SEC profile of the soluble fraction of polycaryophyllene crosslinked by BPO.

**Figure S8.** FTIR Analysis of (a) polycaryophyllene and cross-linked polycaryophyllene by (b) DCP, (c) BPO, (d) SS.

**Figure S9.** Online curing of polycaryophyllene by BPO followed by rheology.

**Figure S10.** Online curing of polycaryophyllene by SS followed by rheology.

**Figure S11.** DSC online curing measurement of polycaryophyllene by DCP.

**Figure S12.** DSC online curing measurement of polycaryophyllene by BPO.

**Table S2.** Gel fractions of cross-linked polycaryophyllene by different thiols.

**Figure S13.** FTIR Analysis of (a) polycaryophyllene and cross-linked polycaryophyllene by HDT with 0.5eq and 1 eq. of SH per double bond.

**Figure S14.** FTIR Analysis of (a) polycaryophyllene and cross-linked polycaryophyllene by dithiols with 1 eq. of SH per double bond.

**Figure S15.** TGA and DTG curves of polycaryophyllene, and cross-linked polycaryophyllene by EDT, BDT, HDT, DDT. (0.5 equiv SH to DB.)

**Figure S16.** TGA and DTG curves of cross-linked polycaryophyllene BPO.

**Figure S17.** DSC curves of polycaryophyllene pure, and cross-linked polycaryophyllene by EDT, BDT, HDT, DDT with 0.5 of thiol per double bond.

**Figure S18.** DSC curves of polycaryophyllene pure, and cross-linked polycaryophyllene by EDT, BDT, HDT, DDT with 1 equiv. of thiol per double bond.

**Figure S19.** DMA analysis of cross-linked polycaryophyllene by EDT, BDT, HDT, DDT (0.5 eq. of SH per db). Storage modulus ( $E'$ ) in solid line,  $\tan \delta$  in dashed line.

**Figure S20.** Tensile strength and elongation at break of cross-linked polycaryophyllene by SS, BPO, and DDT 0.5 equiv.

**Table S3.** General properties of different polyterpenes.

## S1. General experimental procedure

Caryophyllene ( $\geq 80\%$ ), Grubbs' 2<sup>nd</sup> Generation catalyst ((tricyclohexylphosphine) (1.3-dimesitylimidazolidine-2-ylidene) benzylideneruthenium dichloride), dicumyl peroxide (DCP, 98%), IRGARCUR 2959, 1,2-ethanedithiol (EDT), 1,4-butanedithiol (BDT), 1,6-hexanedithiol (HDT), and 1,10-decanedithiol (DDT), dichloromethane and tetrahydrofuran were purchased from Sigma-Aldrich. Benzoyl peroxide (BPO, 75%) was purchased from Fischer Scientific. Sulfur curing system i.e. sulfur, zinc oxide, stearic acid and N-tert-butyl-2-benzothiazyl sulfenamide (TBBS) accelerator were supplied by EMAC company. All products and solvents (reagent grade) were used as received.

### *i) Synthesis of polycaryophyllene*

The synthesis of polycaryophyllene was based on Grau's procedure. The caryophyllene was placed into a Schlenk flask in which 0.2 wt. % of Grubbs catalyst 2<sup>nd</sup> generation ( $C_{46}H_{65}Cl_2N_2PRu$ ) was added under nitrogen atmosphere. The reaction was conducted for 24 h at room temperature. The scheme of the reaction is depicted in the figure below.

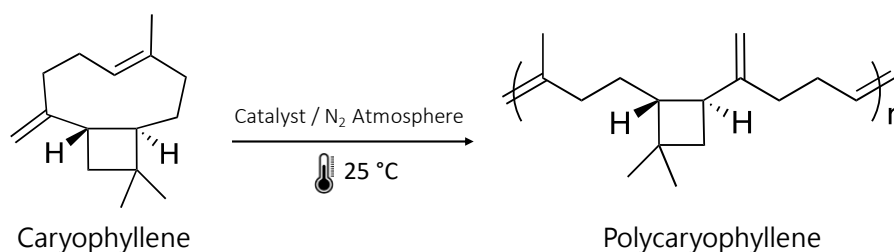


**Figure S1** Schematic reaction of the polymerization of caryophyllene.

A sticky polymer was obtained at the end and used without any further purification. The product was characterized by <sup>1</sup>H NMR, SEC and DSC, which are shown in Figs **S4**, **S5**, **S6**.

### *ii) Cross-linking of polycaryophyllene using thermosensitive cross-linkers*

1) Organic peroxide: The polycaryophyllene and cross-linking agent (15 wt. %) were homogenized and placed in a machine press. The mixture was kept in the machine press for 1 h at 160°C under 30 bar.

2) Vulcanization by sulfur system: The polycaryophyllene and sulfur system (2 phr of ZnO, 2 phr of stearic acid, 3 phr of sulfur, and 15 phr of TBBS accelerator) were homogenized and placed in a machine press. The mixture was kept in the machine press for 1 h at 160°C under 30 bar. At the end, a rubber-like cross-linked polymer was obtained.

*iii) Photocross-linking of polycaryophyllene under UV light radiation*

The cross-linking reactions under UV radiation were carried out in a reactor equipped with a UV lamp ( $\lambda = 320\text{-}380\text{ nm}$ ). The polycaryophyllene, IRGARCUR 2959 (0.02 equiv.), selected dithiol (0.25 or 0.5 equiv. to double bonds) and dichloromethane (3 mL) were homogenized and placed in a Teflon mould. The teflon mould was left overnight to evaporate the solvent. Then, the mixture was dried under vacuum for 4 hours to make sure that all solvent was removed. The Teflon mold was thus enclosed into the UV-reactor for 5h at room temperature. At the end, a film-like was obtained. In this study, thiols with different carbon chains were used 1,2-ethanedithiol (EDT), 1,4-butanedithiol (BDT), 1,6-hexanedithiol (HDT), and 1,10-decanedithiol (DDT) (Figure 1).

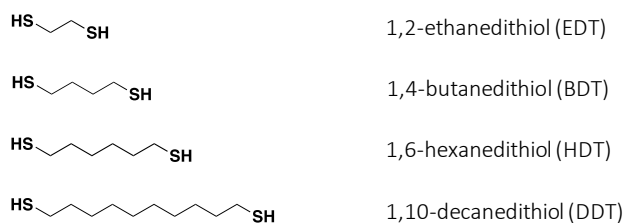


**Figure S2** Chemical structures of different thiols.

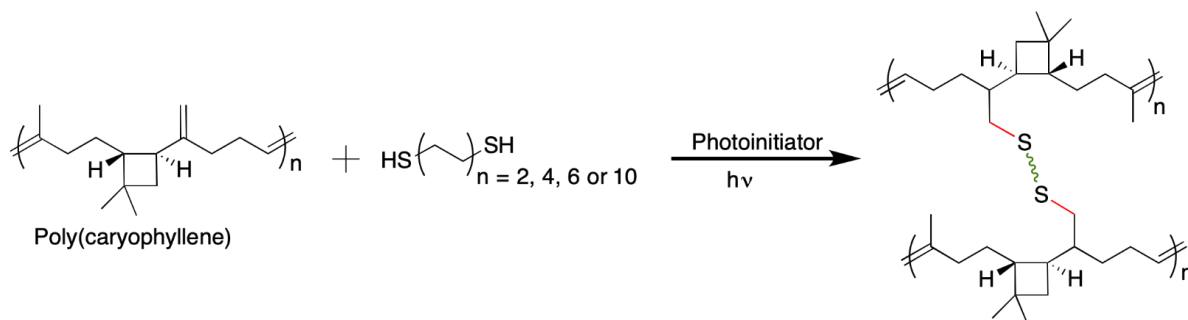


**Figure S3** Thiol-ene cross-linking reaction of polycaryophyllene.

#### *iv) Characterizations*

NMR spectra were recorded using a Bruker AC-400 NMR, at room temperature, in deuterated chloroform ( $\text{CDCl}_3$ ).

Fourier Transform Infrared (FT-IR) spectra were performed on a Bruker VERTEX 70 spectrometer equipped with diamond crystal (GladiATR PIKE technologies) for the attenuated total reflection (ATR) mode. The spectra were acquired from 400 to 4000  $\text{cm}^{-1}$  at room temperature using 32 scans at a resolution of 4  $\text{cm}^{-1}$ .

Polymer molar masses were determined by size exclusion chromatography (SEC) using tetrahydrofuran (THF with 250 ppm of BHT as an inhibitor) as an eluent and trichlorobenzene as a flow marker. Measurements in THF were performed on a ThermoFisher Scientific Ultimate 3000 system equipped with Diode Array Detector, Wyatt light scattering detector and RI detector. The separation was achieved on three Tosoh TSK gel columns: G4000HXL (particles of 5 mm, pore size of 200 Å, exclusion limit of 400 000  $\text{g mol}^{-1}$ ), G3000HXL (particles of 5 mm, pore size of 75 Å, exclusion limit of 60 000  $\text{g mol}^{-1}$ ), G2000HXL (particles of 5 mm, pore size of 20 Å, exclusion limit of 10 000  $\text{g mol}^{-1}$ ), at flow rate of 1  $\text{mL min}^{-1}$ . The injected volume was 20  $\mu\text{L}$ . Columns' temperature was held at 40 °C. Data were recorded and processed by Astra software from Wyatt. SEC was calibrated using polystyrene standards.

The rheology measurements were performed on an Anton Paar MCR302 controlled-stress rheometer and frequency was modulated at 6.28  $\text{rad.s}^{-1}$  with a shear strain ( $\gamma$ ) variation of 1%. The measurements of  $G'$  and  $G''$  were performed as a function of temperature from 30°C to 160 °C at a rate of 10°C.min<sup>-1</sup>. The polycaryophyllene and cross-linker were previously homogenized and then placed between two plates of 8 mm diameter. Finally, the temperature was maintained at 160 °C for 30 minutes.

Thermogravimetric analysis (TGA) thermograms were obtained using a TGA Q500 apparatus from TA instruments. Samples (~10 mg) were heated from room temperature to 700 °C at a rate of 10 °C min<sup>-1</sup> under nitrogen atmosphere.

Differential scanning calorimetry (DSC) measurements of samples (~5 mg) were performed using a DSC Q 100 apparatus from TA Instruments over temperature range from -120 °C to 240 °C, in a heating-cooling mode of 10 °C min<sup>-1</sup>. The analyses were carried out in a helium atmosphere using aluminum pans. Glass transition temperatures and melting points were obtained from the second heating runs.

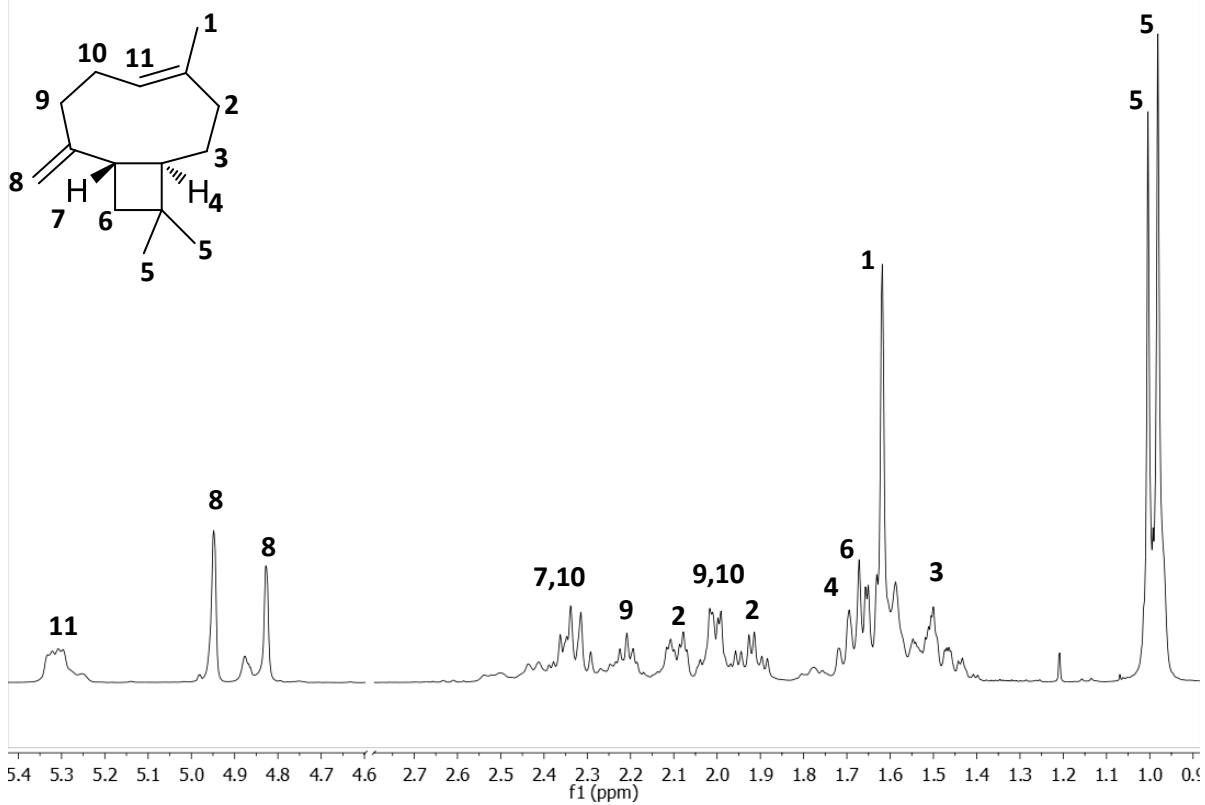
Dynamic mechanical analysis (DMA) measurements were carried out using a RSA3 apparatus from TA Instruments equipped with a liquid nitrogen cooling system. The thermomechanical properties of the samples (width  $\cong$  5 mm; thickness  $\cong$  2 mm and length of the fixed section  $\cong$  10 mm) were studied from around -50 °C to 60°C at a heating rate of 3 °C min<sup>-1</sup>. The measurements were performed in tensile test at a frequency of 1 Hz, a strain sweep of 0.03% and an initial static force of 0.1 N.

Tensile tests were performed on extension mode test system using RSA3 apparatus from TA instruments. The measurements were carried out at room temperature for rectangular samples (width  $\cong$  5 mm; thickness  $\cong$  2 mm) using a cross-head speed of 2 mm.min<sup>-1</sup>.

The gel fractions were calculated by using the equation  $GF = \frac{w_d}{w_0} \cdot 100\%$ , where  $w_d$  is the mass of the dried sample and  $w_0$  is the mass of the sample before swelling test.

The cross-link densities ( $\nu$ ) of networks defined as the number of moles of elastically effective network chains per cubic centimetre of sample which can be calculated with the following equation with  $R = 8,314 \text{ J.mol}^{-1}.\text{K}^{-1}$ ,  $T_{\alpha+30}$  and  $\phi = 1$ .  $\nu = \frac{E'(T_{\alpha+30})}{\phi \cdot R \cdot T_{\alpha+30}}$  (2)

121025egrau-51-EG-caryo99 PROTON128 CDCl3 /DATA/topspin egrau 51



121025egrau-51-EG-caryo99 CARBON\_1024scans CDCl3 /DATA/topspin egrau 51

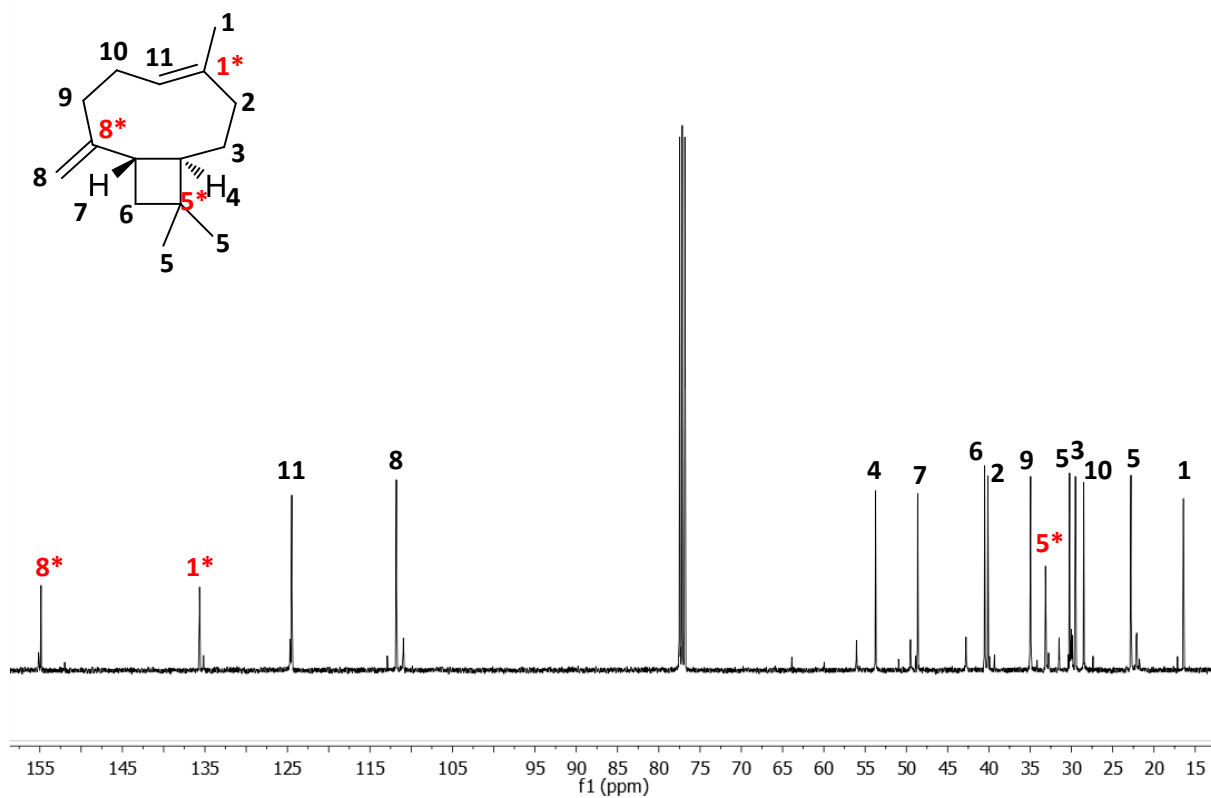
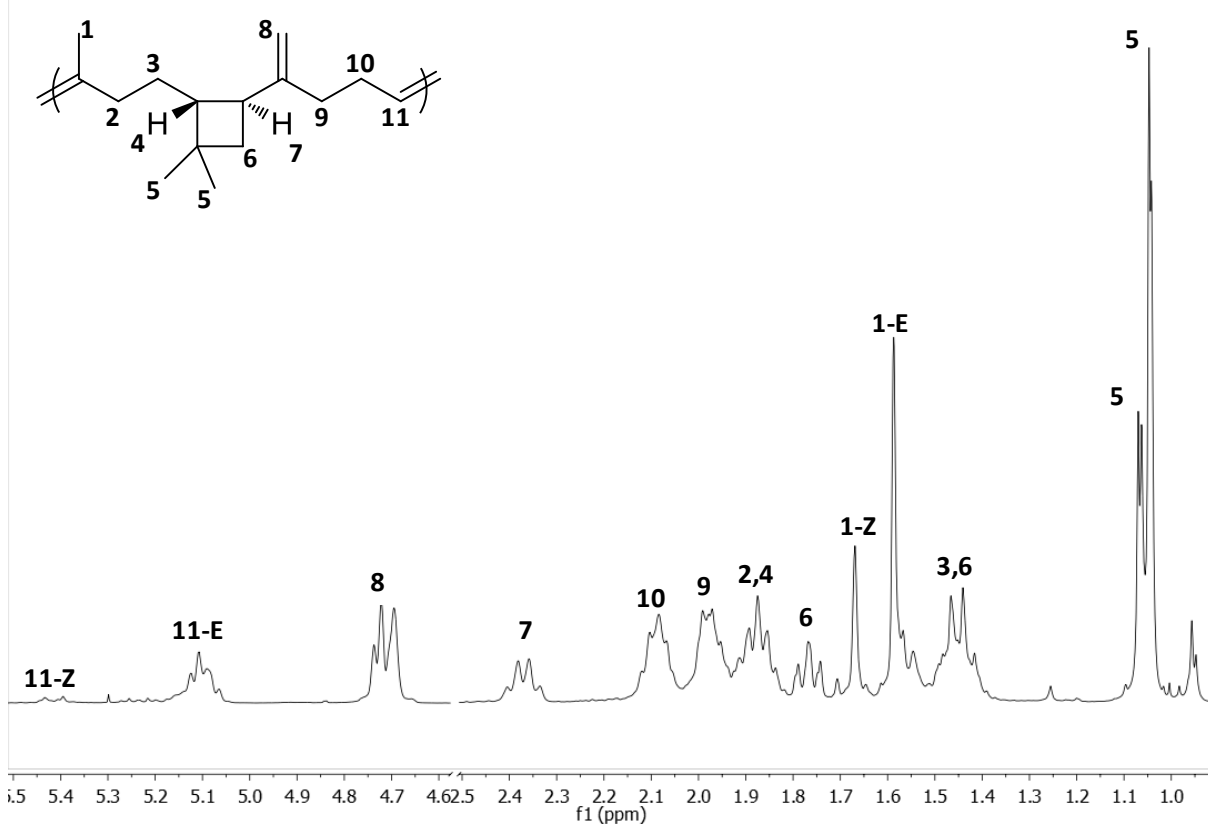


Figure S4: <sup>1</sup>H and <sup>13</sup>C NMR spectrum of caryophyllene in CDCl<sub>3</sub>

121025egrau-54-EGPolycaryoG3 PROTON128 CDCl3 /DATA/topspin egrau 54



121025egrau-54-EGPolycaryoG3 CARBON\_1024scans CDCl3 /DATA/topspin egrau 54

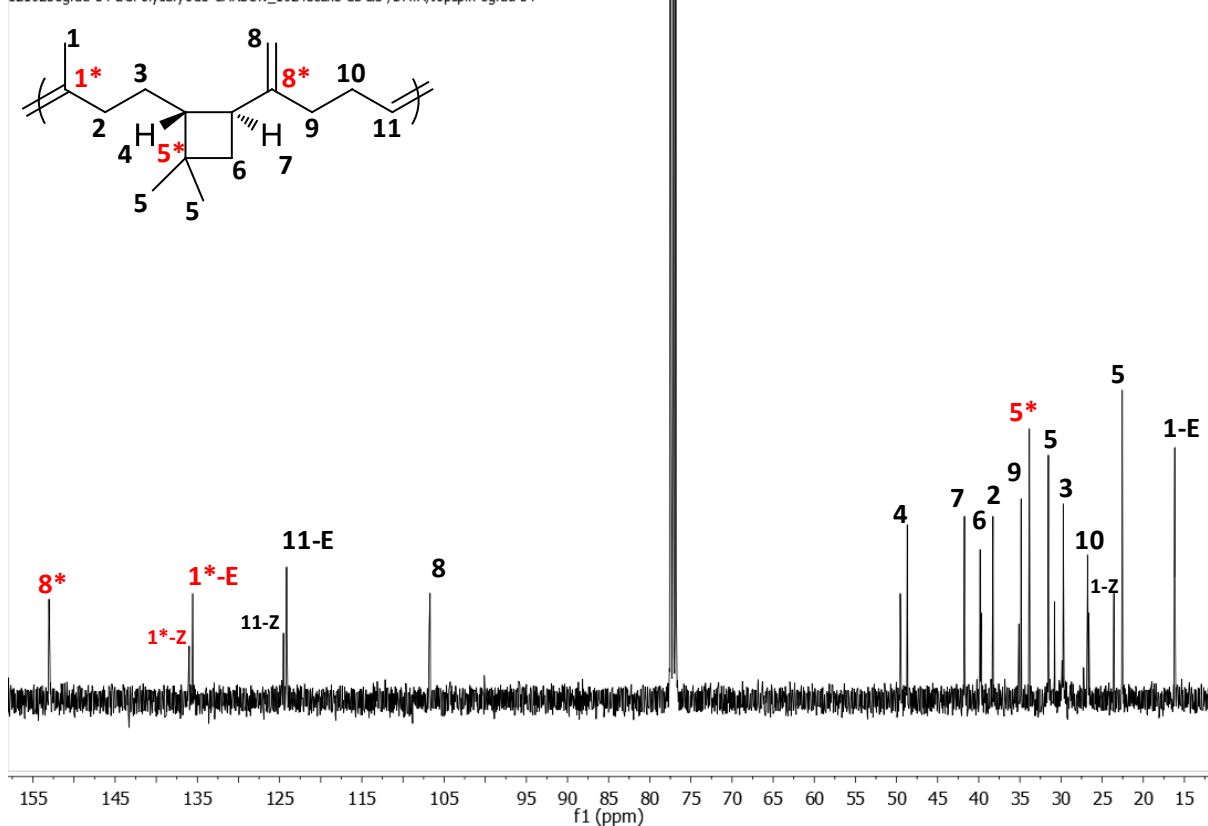
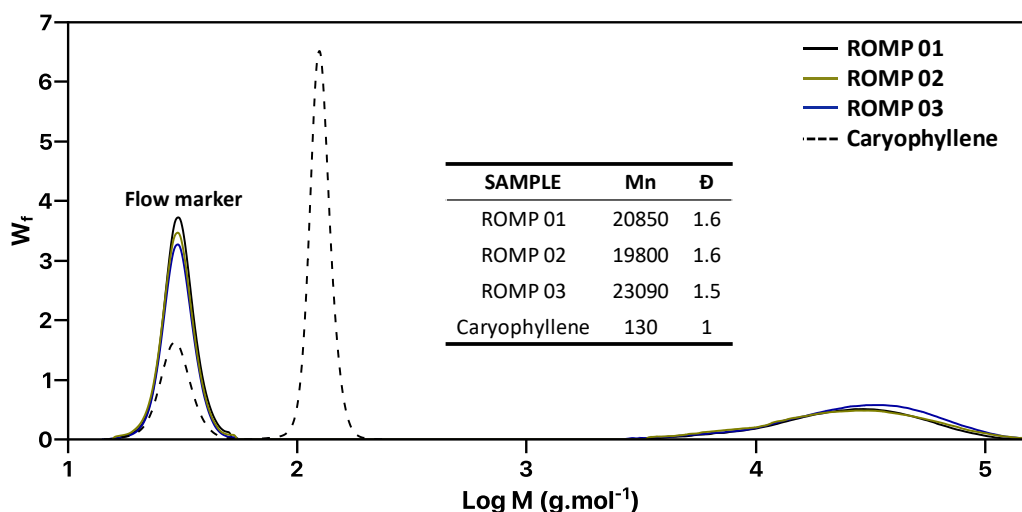


Figure S5 <sup>1</sup>H and <sup>13</sup>C NMR spectrum of polycaryophyllene in CDCl<sub>3</sub>.



**Figure S6** Three different samples of Polycaryophyllene and Caryophyllene SEC profile. ROMP 01-03 were performed using 5, 50, and 50g of caryophyllene respectively

**Table S1** Gel fractions of cross-linked polycaryophyllene by BPO at varied temperatures.

| Curing temperature<br>by BPO | Gel Fraction<br>(%) |
|------------------------------|---------------------|
|                              | 15 wt. %            |
| 100 °C                       | 27                  |
| 120 °C                       | 36                  |
| 140 °C                       | 43                  |
| 160 °C                       | 64                  |
| 170 °C                       | 63                  |
| 180 °C                       | 60                  |

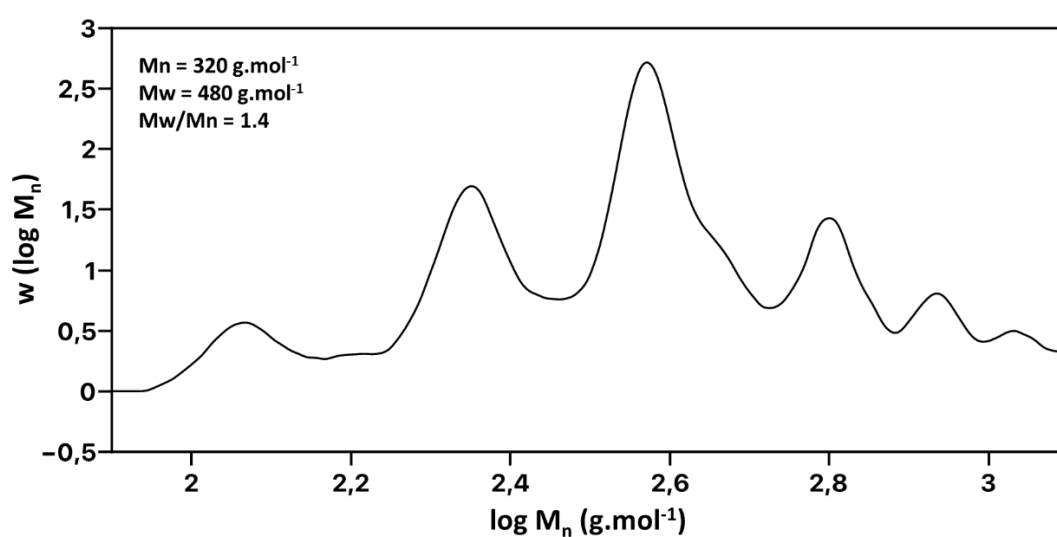


**Figure S7** SEC profile of the soluble fraction of polycaryophyllene crosslinked by BPO.

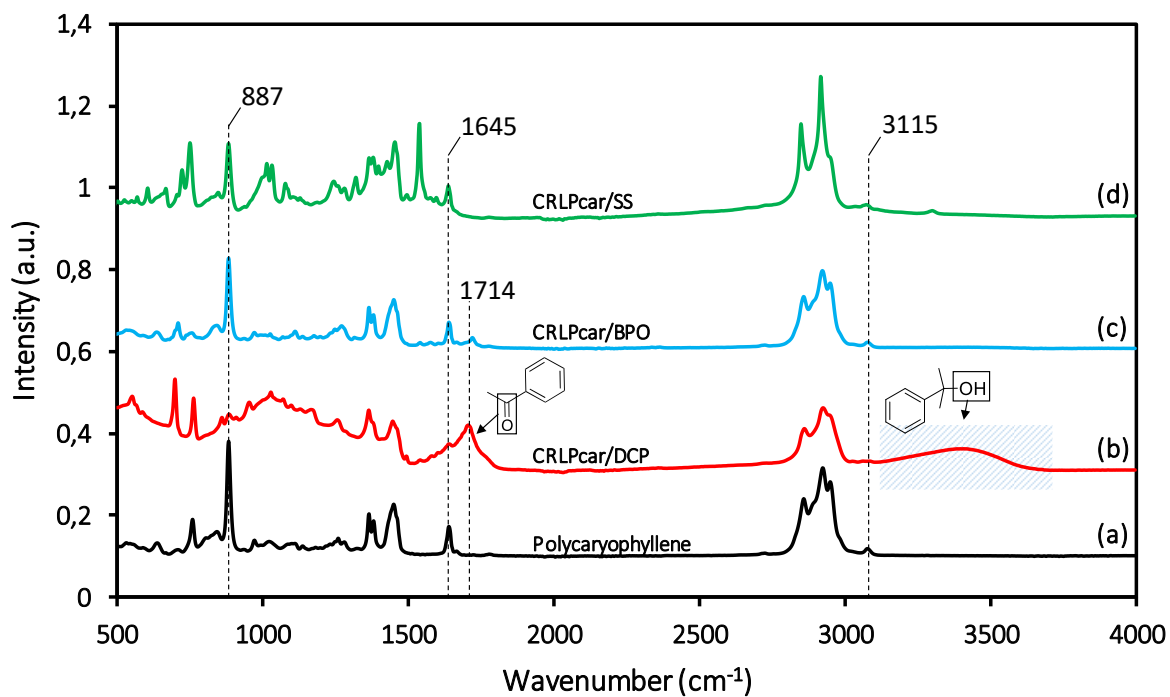


Figure S8 FTIR Analysis of (a) polycaryophyllene and cross-linked polycaryophyllene by (b) DCP, (c) BPO, (d) SS.

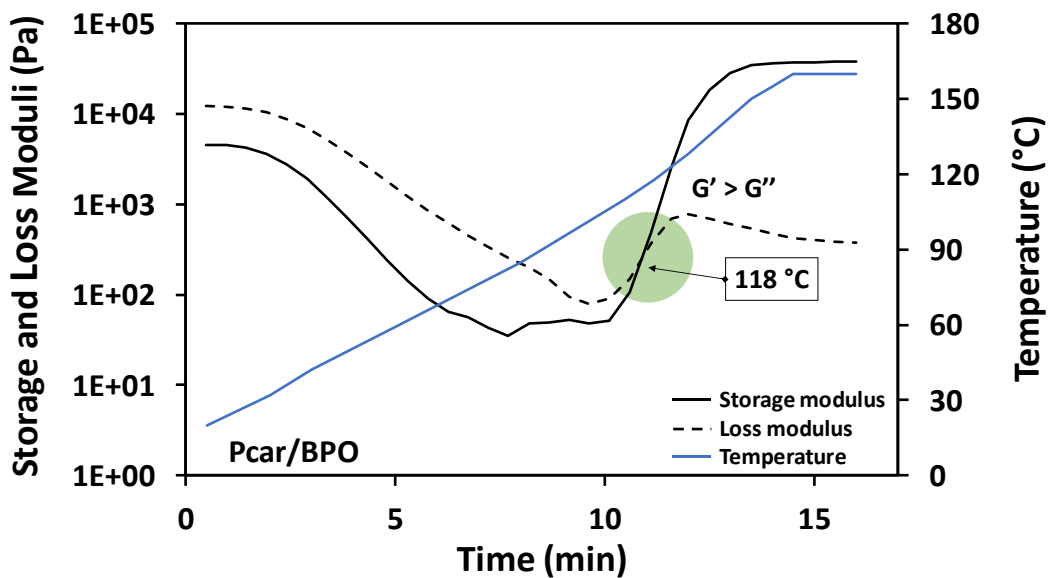


Figure S9 Online curing of polycaryophyllene by BPO followed by rheology.

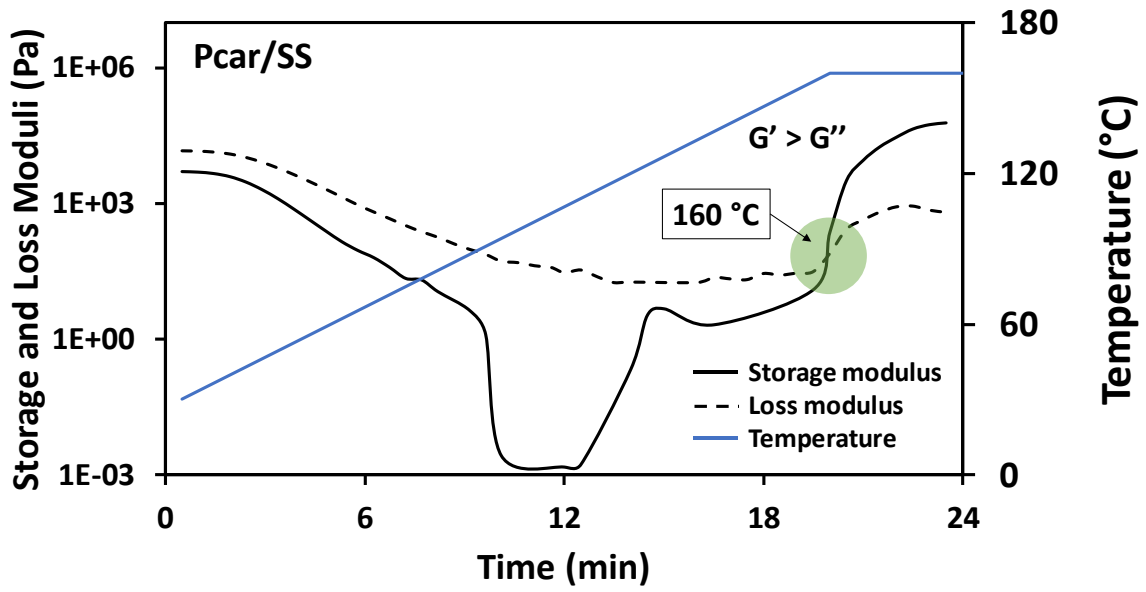


Figure S10 Online curing of polycaryophyllene by SS followed by rheology.

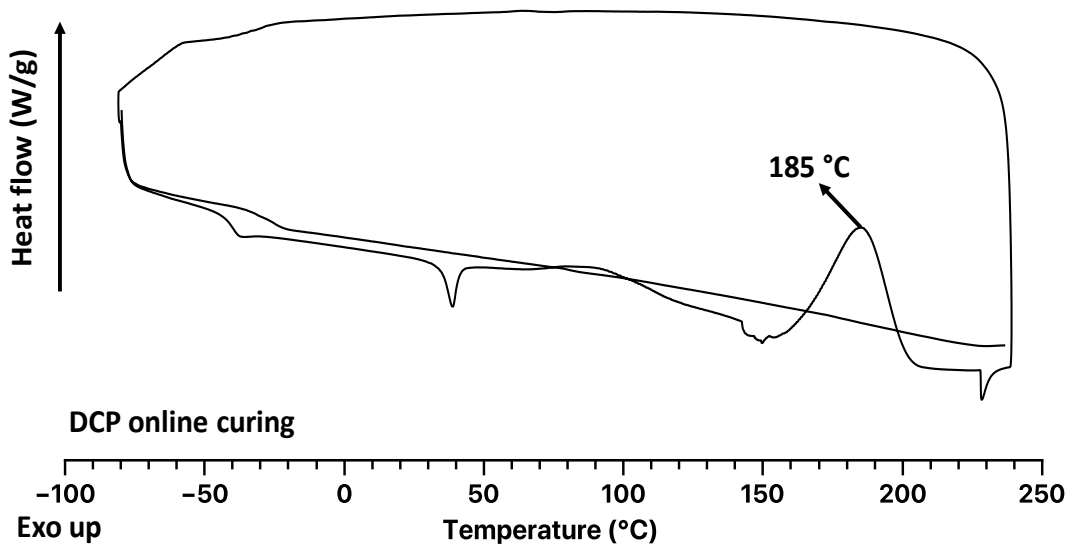
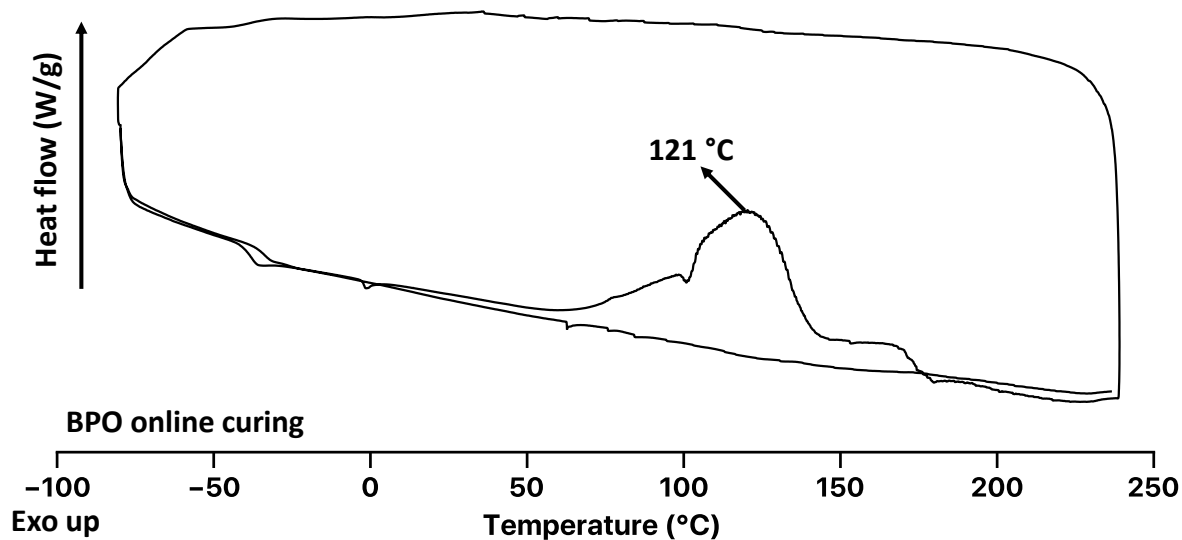


Figure S11 DSC online curing measurement of polycaryophyllene by DCP.



**Figure S12** DSC online curing measurement of polycaryophyllene by BPO.

**Table S2** Gel fractions of cross-linked polycaryophyllene by different thiols.

| <i>Dithiol</i> | <i>Gel content (%)</i>        |                             |
|----------------|-------------------------------|-----------------------------|
|                | 0.5 eq. of SH per double bond | 1 eq. of SH per double bond |
| <i>EDT</i>     | 100                           | 100                         |
| <i>BDT</i>     | 100                           | 90                          |
| <i>HDT</i>     | 95                            | 94                          |
| <i>DDT</i>     | 98                            | 89                          |

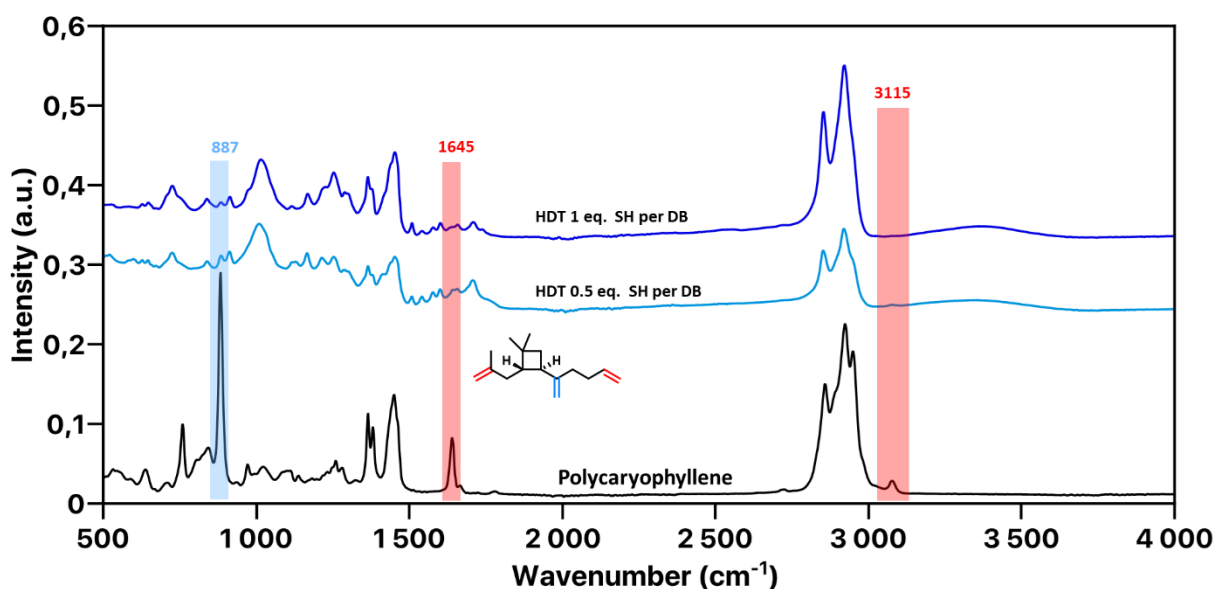


**Figure S13** FTIR Analysis of (a) polycaryophyllene and cross-linked polycaryophyllene by HDT with 0.5eq and 1 eq. of SH per double bond.

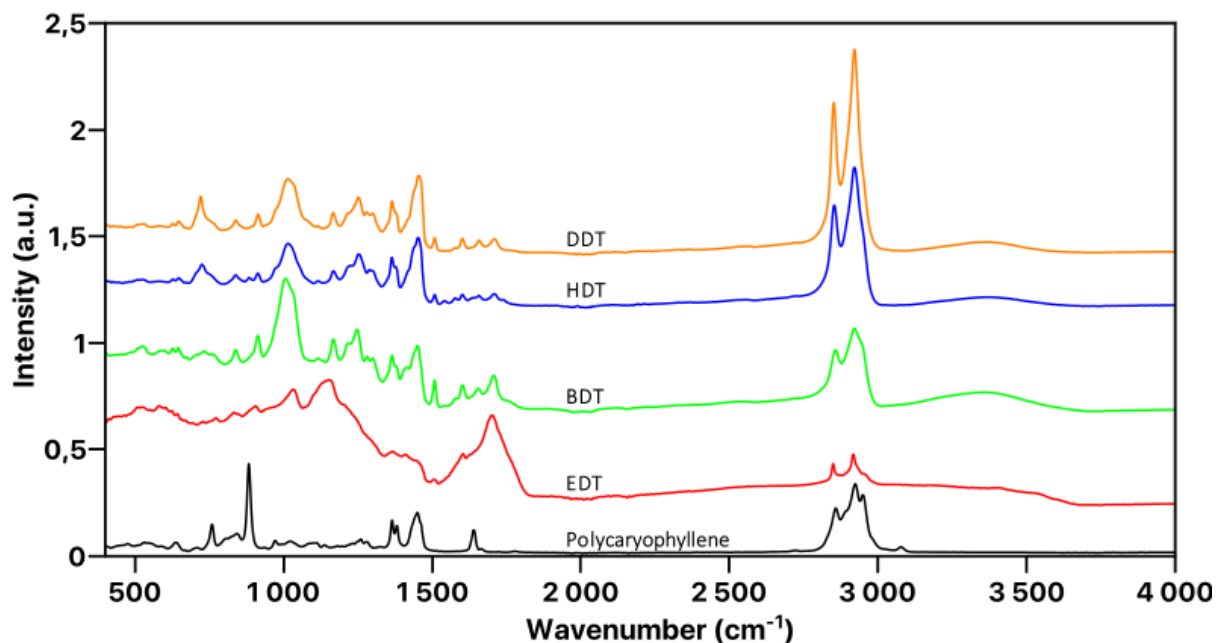


**Figure S14** FTIR Analysis of (a) polycaryophyllene and cross-linked polycaryophyllene by dithiols with 1 eq. of SH per double bond.

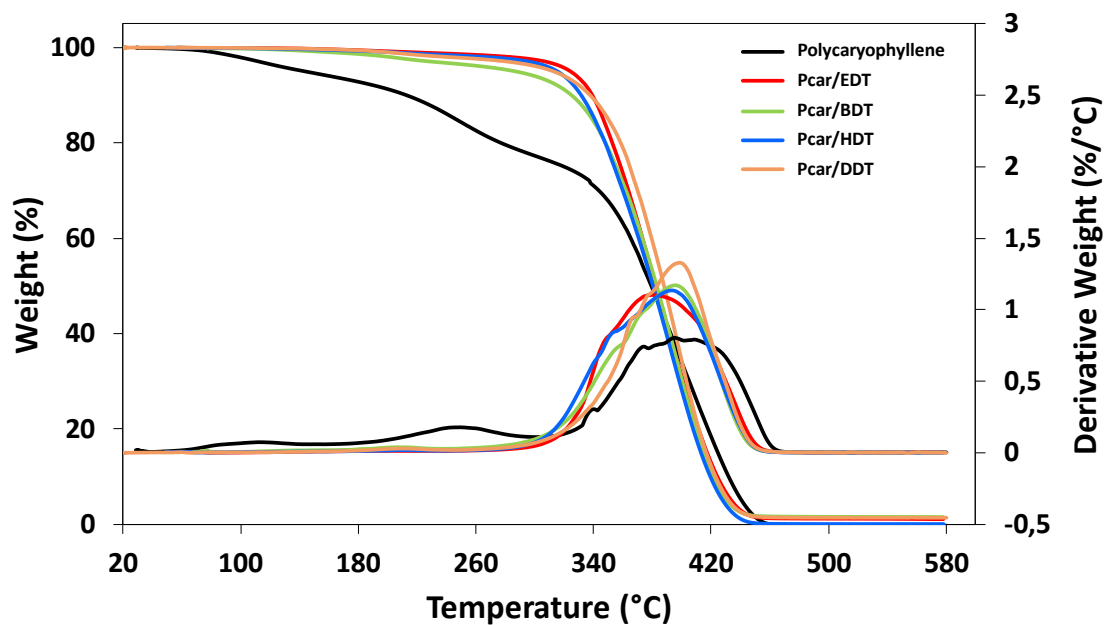


**Figure S15** TGA and DTG curves of polycaryophyllene, and cross-linked polycaryophyllene by EDT, BDT, HDT, DDT. (0.5 equiv SH to DB.)

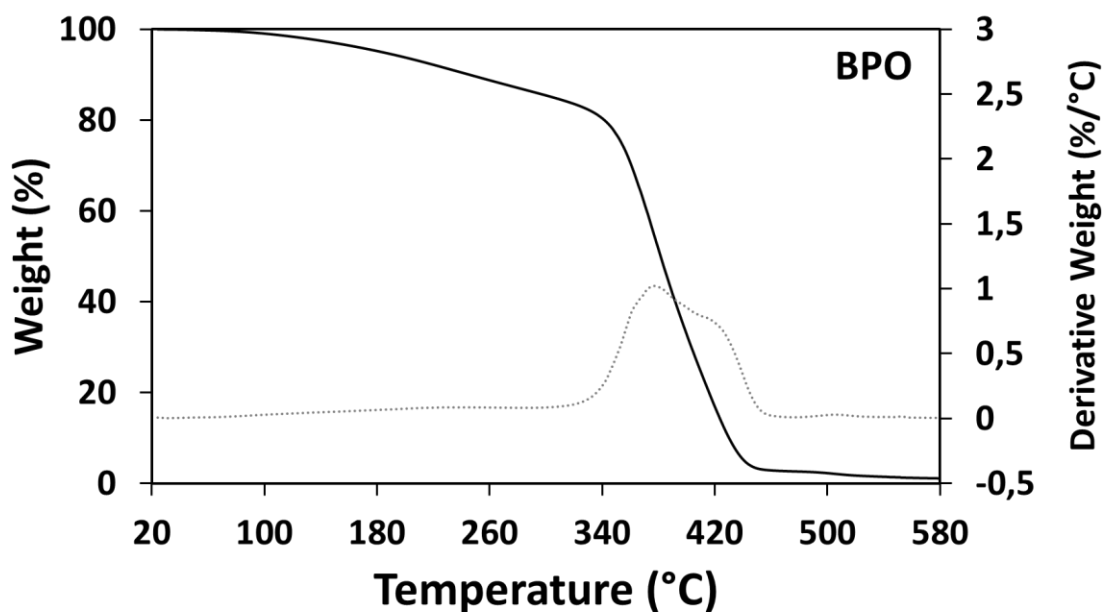


Figure S16 TGA and DTG curves of cross-linked polycaryophyllene BPO.

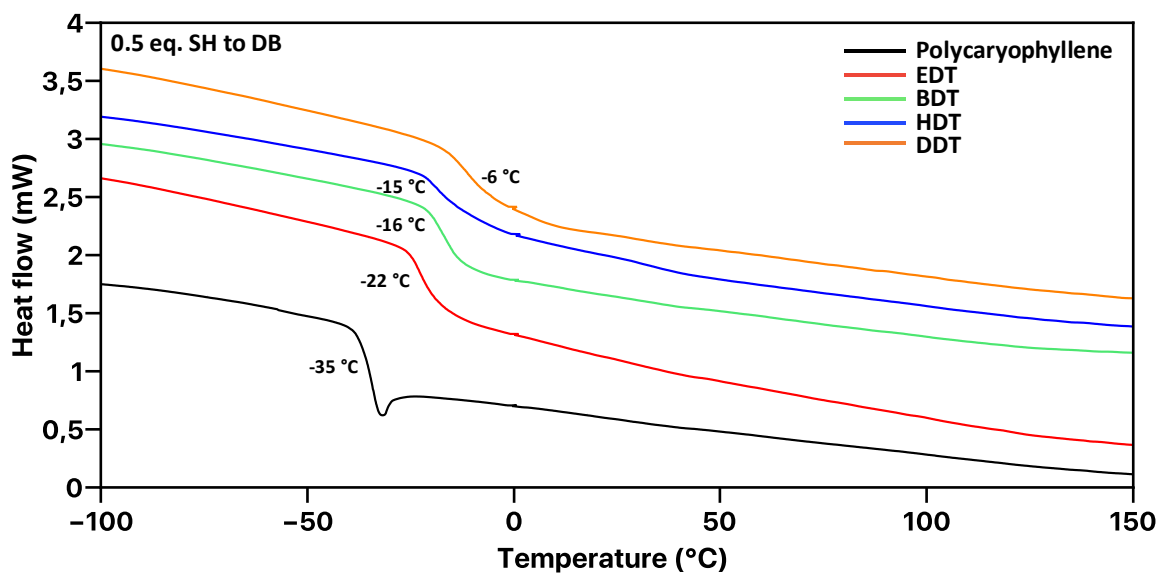
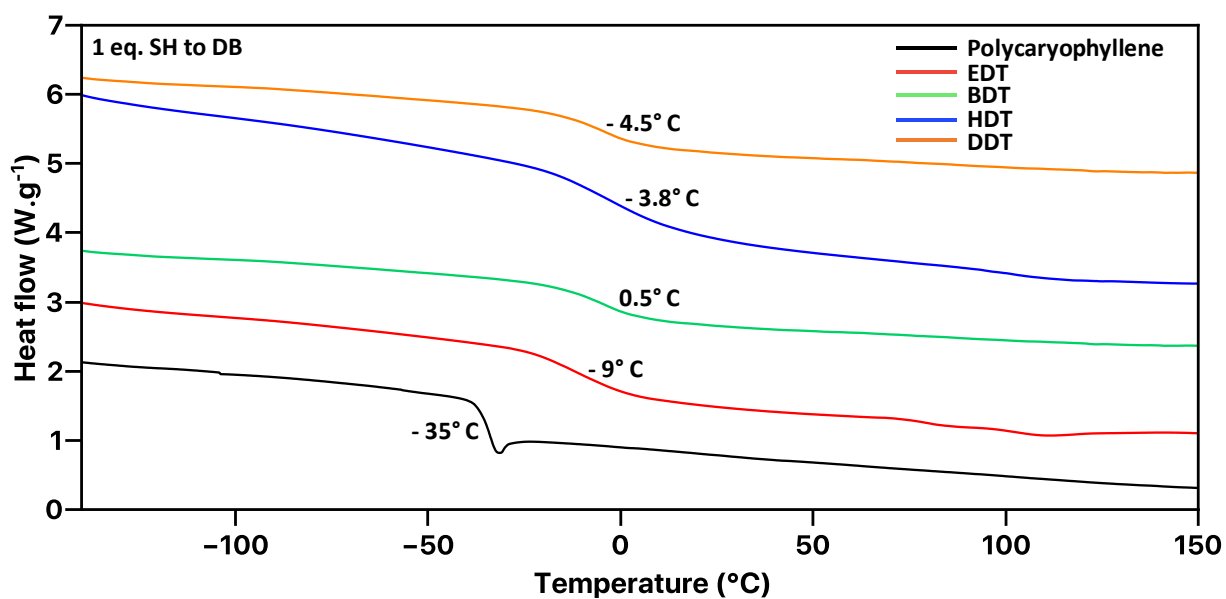
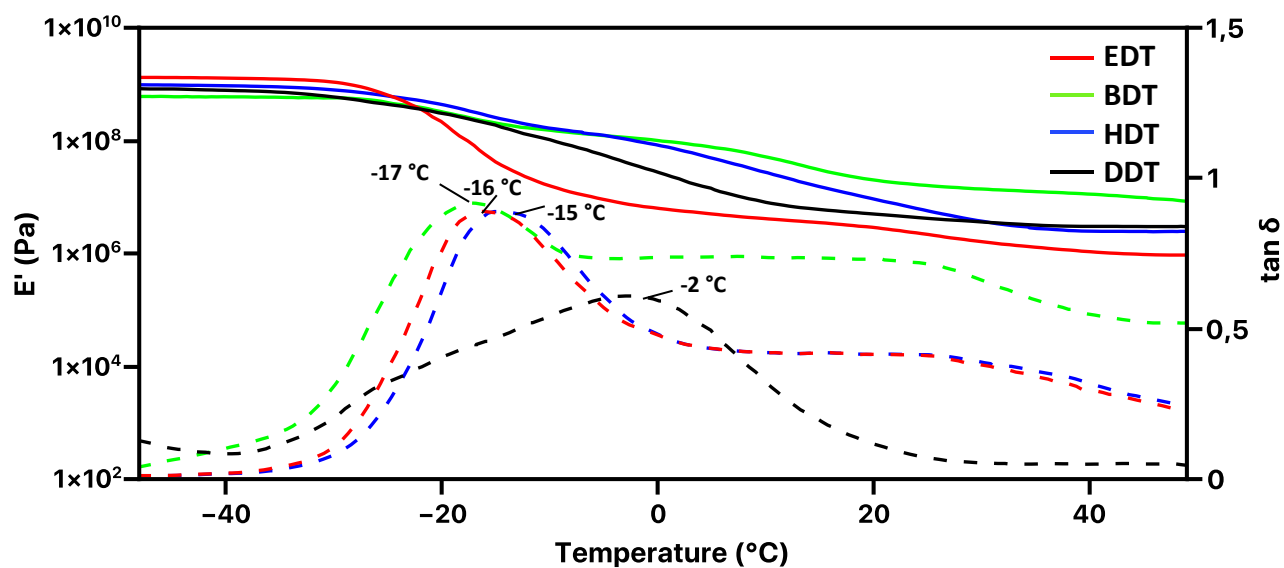


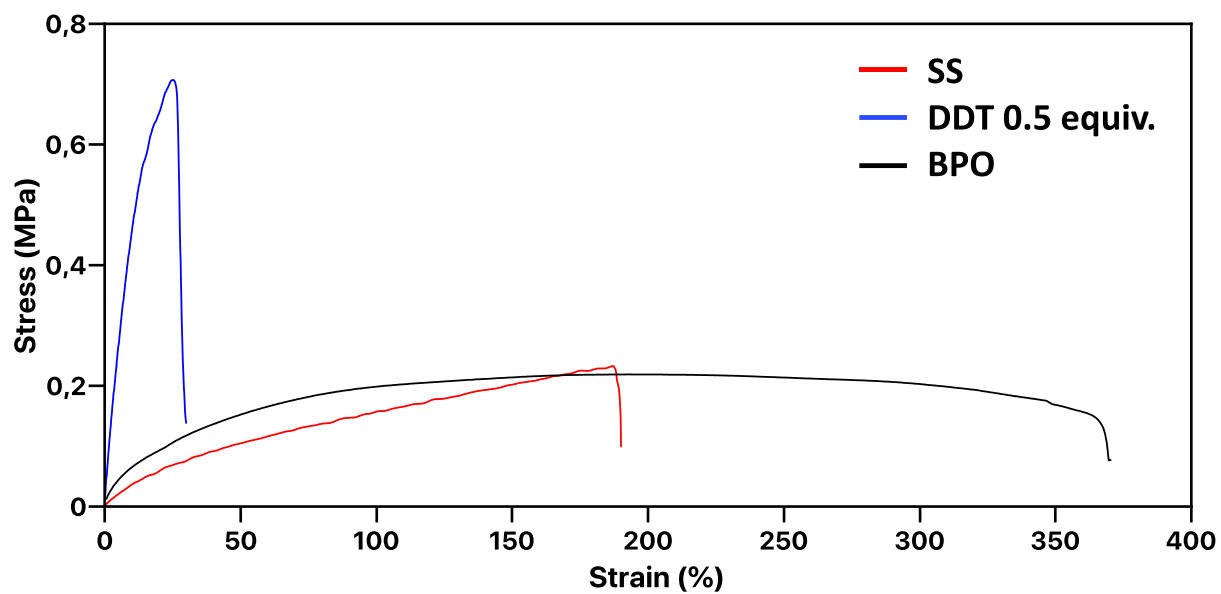
Figure S17 DSC curves of polycaryophyllene pure, and cross-linked polycaryophyllene by EDT, BDT, HDT, DDT with 0.5 of thiol per double bond.



**Figure S18** DSC curves of polycaryophyllene pure, and cross-linked polycaryophyllene by EDT, BDT, HDT, DDT with 1 equiv. of thiol per double bond.

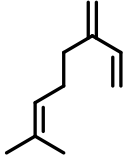
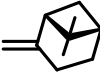
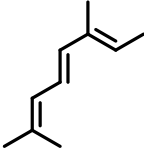
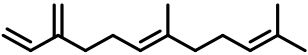
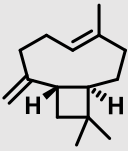


**Figure S19** DMA analysis of cross-linked polycaryophyllene by EDT, BDT, HDT, DDT (0.5 eq. of SH per db). Storage modulus ( $E'$ ) in solid line,  $\tan \delta$  in dashed line.



**Figure S20** Tensile strength and elongation at break of cross-linked polycaryophyllene by SS, BPO, and DDT 0.5 equiv.

**Table S3.** General properties of different polyterpenes.

| Terpene Unit  | Polymerization method                     | $T_g$ (°C) | Molar mass (g.mol <sup>-1</sup> ) | Reference |
|---|---|------------|-----------------------------------|-----------|
|    | Free Radical<br>Poly( $\beta$ -myrcene)   | -73        | $9 \times 10^4$                   | 19        |
|    | Cationic<br>Poly( $\beta$ -pinene)        | 90         | $4 \times 10^4$                   | 23        |
|   | Free Radical<br>Poly-allocimene           | -17        | $1 \times 10^4$                   | 18        |
|  | Anionic<br>Poly( $\beta$ -farsene)        | -70        | $1 \times 10^4$                   | 25        |
|  | Free Radical<br>Polylimonene              | 116        | $4 \times 10^4$                   | 24        |
|  | Cationic<br>Poly( $\alpha$ -phellandrene) | 130        | $1 \times 10^4$                   | 24        |
|  | ROMP<br>Poly(caryophyllene)               | -35*       | $2 \times 10^4$                   | This work |